Diagn Interv Radiol 2023; DOI: 10.4274/dir.2023.221932

MODALITY-BASED (UC, CT, MRI, PET-CT) IMAGING

ORIGINAL ARTICLE

The role of (^{18}F)-fluoro-D-glucose positron emission tomography/computed tomography in the surveillance of abnormal myocardial energy metabolism and cardiac dysfunction in a rat model of cardiopulmonary resuscitation

Liming Pan
Fan Zhang
Yingqi Ran
Lei Bi
Hongjun Jin
Lan Yao

PURPOSE

To investigate the feasibility and usefulness of 2-deoxy-2-(^{18}F)-fluoro-D-glucose positron emission tomography/computed tomography [(^{18}F)-FDG PET/CT] as a novel examination in the surveillance of abnormal myocardial energy metabolism and cardiac dysfunction after cardiopulmonary resuscitation (CPR).

METHODS

Thirteen male Sprague–Dawley rats were randomly divided into a sham group (n = 4), CPR group (n = 4), and trimetazidine (TMZ) + CPR group (n = 5). The expression levels of the myocardial injury marker cardiac troponin I (CTNI) in serum were tested at 6 hours after CPR or TMZ + CPR. The ejection fraction and fraction shortening were evaluated by echocardiography. (^{18}F)-FDG PET/CT was used to measure the FDG uptake and the standardized uptake value (SUV) after CPR or TMZ + CPR for 6 hours. The intermediary carbohydrate metabolites of glycolysis including phosphoenolpyruvate, 3-phospho-D-glycerate, and the lactate/pyruvate ratio were detected through the multiple reaction monitoring approach. Simultaneously, the authors also tested the expression levels of the total adenosine triphosphate (ATP) and the key intermediate products of glucose ovidation as alpha ketoglutarate, citrate, and succinate in the myocardium.

RESULTS

The authors found that the aerobic oxidation of glucose was reduced, and the anaerobic glycolysis was significantly enhanced in the myocardium in the early stage of CPR. Meanwhile, the myocardial injury marker CTNI was upregulated considerably ($P = 0.014$, $P = 0.021$), and the left ventricular function of the animal heart also markedly deteriorated with the downregulation of ATP after CPR. In contrast, myocardial injury and cardiac function were greatly improved with the increase of ATP in the CPR + TMZ group. In addition, aerobic glucose oxidation metabolites were significantly increased ($P < 0.05$) and anaerobic glycolysis metabolites were significantly decreased ($P < 0.05$) after CPR in the myocardium. Surprisingly, (^{18}F)-FDG PET/CT could track the above changes by detecting the FDG uptake value and the SUV.

CONCLUSION

Glucose metabolism is an essential factor for myocardial self-repair after CPR. (^{18}F) FDG PET/CT, as a non-invasive technology, can monitor myocardial energy metabolism and cardiac function by tracking changes in glucose metabolism after CPR.

KEYWORDS

Cardiac function, cardiopulmonary resuscitation, glucose metabolism, myocardial energy metabolism, (^{18}F)-FDG PET/CT

From the Department of Emergency (L.P., F.Z., Y.R., L.Y. ✉yaolan2@mail.sysu.edu.cn), the Fifth Affiliated Hospital, Sun Yat-Sen University, Zhuhai, China; Key Laboratory of Biomedical Imaging (L.B., H.J.), Fifth Affiliated Hospital, Sun Yat-Sen University, Zhuhai, China.

Received 02 October 2022; revision requested 31 January 2023; accepted 26 March 2023.

Epub: 08.05.2023

Publication date: 30.05.2023

DOI: 10.4274/dir.2023.221932

You may cite this article as: Pan L, Zhang F, Ran Y, Bi L, Jin H, Yao L. The role of (^{18}F)-fluoro-D-glucose positron emission tomography/computed tomography in the surveillance of abnormal myocardial energy metabolism and cardiac dysfunction in a rat model of cardiopulmonary resuscitation. *Diagn Interv Radiol.* 2023;29(3):548-554.

Myocardial dysfunction remains a leading problem in the early period following the return of spontaneous circulation (ROSC) after cardiac arrest. Post-resuscitation myocardial injury is evidently due to oxidative stress, calcium overload, neutrophil accumulation, microvascular damage, and abnormal energy metabolism, among other causes.[1-3] As one of the most common pathological mechanisms after the ROSC, energy metabolism disorder in the myocardium leads to a series of detrimental changes in the energy supply and substrate metabolism related to the regulation of mitochondrial function, oxidative stress, and inflammation.[4,5]

Glucose and fatty acids are important energy substrates for myocardial metabolism.[6] Sixty to seventy percent of the energy required for cardiac contraction under normal physiological conditions is mainly furnished by the oxidative metabolism of fatty acids, with the remainder predominantly from glucose.[7] The metabolism of fatty acids and glucose undergoes adaptive changes in the myocardium due to ischemia-reperfusion injury after cardiopulmonary resuscitation (CPR). The rate of aerobic oxidation of free fatty acids and glucose in cardiomyocytes is decreased, yet the rate of anaerobic glycolysis is enhanced.[8,9] Glucose anaerobic metabolism becomes progressively more mainstream in the heart after the ROSC. Some *in vitro* experiments demonstrated that early intervention in cardiac metabolism disorder attenuated myocardial damage and dysfunction. Therefore, it is crucial in the clinical setting to detect myocardial metabolism conditions in real-time to evaluate the latent cardiac injury and make optimum treatment plans during the ROSC. Nevertheless, there is no proven technique to track cardiac metabolism changes after CPR.

2-deoxy-2-(^{18}F)-fluoro-D-glucose [(^{18}F)-FDG], as an analog of glucose, is transported into the cell by facilitated diffusion and is phosphorylated to (^{18}F)-FDG-6-phosphate.[10]

Main points

- Impaired energy metabolism was closely related to myocardial damage after cardiopulmonary resuscitation (CPR).
- Abnormal glycolysis is an important manifestation of myocardial damage after CPR.
- (^{18}F)-fluoro-D-glucose positron emission tomography/computed tomography can be used to evaluate myocardial damage after CPR by monitoring abnormal glucose metabolism.

Once inside the cardiac myocyte, (^{18}F)-FDG-6-phosphate is not metabolized further and has the potential to track glucose uptake and glycolysis.[11-14] The glucose analog 2-(^{18}F)-fluoro-2-deoxy-D-glucose was used to quantify glucose uptake and glycolytic activity in native and transplanted hearts. (^{18}F)-FDG positron emission tomography/computed tomography (PET/CT) has been widely used to identify malignant neoplasms by evaluating aerobic glycolysis conditions in cancer cells. In the present study, the authors investigate whether metabolic disorders of cardiac cells can be traced and detected by (^{18}F)-FDG PET/CT to estimate myocardial impairment and prognosis, given the vital role of abnormal glycolysis in the myocardium after CPR.

Methods

Ethics statement

This study was approved by the Laboratory Animal Management Committee prior to all animal experiments (no: 00053).

Animal model

All rats (males aged 18–20 weeks, bodyweight of 350 ± 25 g) were purchased from the Animal Care and Use Committee. All rats were randomly divided into the sham group (n = 4), CPR group (n = 4), and trimetazidine (TMZ) + CPR group (n = 5). The three groups of animals were fed normal feed for the first two weeks to adapt to the environment, and then the establishment of CPR model animals began. Animals were anesthetized with sodium pentobarbital (45 mg/kg) by intraperitoneal injection and then were subjected to ventilator-assisted breathing (rate of 50 breaths/minute, volume of 0.6 mL/100 g, fraction of inspired oxygen of 0.21). A polyethylene (PE)-50 catheter was inserted from the right carotid artery into the right ventricle. Another PE-50 catheter was inserted into the aorta from the left femoral artery for hemodynamic and arterial pressure monitoring.[15] A 4F PE catheter was inserted into the right external jugular vein and into the right atrium for electrical induction of ventricular fibrillation (VF).

The cardiac rhythm of the rats was monitored by electrocardiogram (ECG) and recorded on ECG drawings. The rats' body temperature was maintained at 36.8 ± 0.2°C throughout the experiment. Hemodynamic data were recorded by a WinDaq data acquisition system (DataQ, Akron, Ohio). Then, the 60 Hz current was gradually increased to a maximum of 3 mAs to the right ventricle endocardium through the guidewire inserted into the right ventricle to induce VF. Mechanical ventilation was stopped, and the induced current was maintained for 8 minutes after the onset of VF. After 8 minutes of untreated VF, CPR (chest compression of 250 beats/minute, with adjustment of chest compression depth by maintaining aortic pressure between 26 and 28 mmHg) and mechanical ventilation (100% oxygen, compression-to-ventilation ratio of 5:1) were started. After 2 minutes of CPR, 0.1 mL of epinephrine (0.1 mg/mL) was injected into the left femoral artery. After 4 minutes of CPR, a 3-J biphasic waveform shock was started at 60-second intervals until the heart rhythm returned to normal. CPR was declared a failure if the rat still had no ROSC after 10 minutes of CPR. After CPR, the rats in the experimental group were given an intraperitoneal injection of TMZ at 10 mg/kg, while the control group was given an intraperitoneal injection. After the ROSC, the oxygen concentration received by the animal through mechanical ventilation gradually decreased from 100% to 21% and was monitored for 3 hours.[16] The ROSC was defined as an organized rhythm with an average aortic pressure of 60 mmHg lasting at least 10 minutes or longer.[17]

Serological testing

Whole blood (200 µL) was collected from rats via the retro-orbital plexuses into Eppendorf tubes containing ethylenediaminetetraacetic acid. The plasma was separated by centrifugation at 4.000 rpm for 15 minutes and stored at -80°C until assayed. The levels of cardiac troponin I (CTNI) were measured using the CTNI Assay Kit according to the manufacturer's instructions.

Echocardiography and hemodynamics

Transthoracic echocardiography (a Vevo 3100 Imaging System with an advanced ultra-high-frequency ultrasound) for small animal research was performed. Then, the left ventricular ejection fraction (EF) and fraction shortening (FS) of the left ventricle were measured. The mean values were obtained from at least three different cardiac cycles.

Targeted myocardial metabolomics analysis

Targeted metabolomics analysis based on the multiple reaction monitoring approach was performed to determine the number of myocardial metabolites. The analysis of targeted energy and glucose metabolism markers was performed by Shanghai Applied Protein Technology Co. Ltd. Briefly, 40 mg

of cardiac tissue was preconditioned with 2000 μL of cool ultrapure water for multi-pass homogenization. Then, 800 μL of pre-cooled methanol/acetonitrile (1:1, v/v) was added, and the mixture was sonicated in an ice bath for 30 minutes and incubated for 1 hour at −20°C to precipitate the proteins. The samples were subsequently centrifuged at 14,000 rcf for 20 minutes at 4°C, and the supernatants were collected. Finally, the analysis of supernatants was performed on an Agilent 1290 Infinity LC system coupled with an AB 5500 QTRAP mass spectrometer in the negative ion mode, followed by the identification and quantification of targeted metabolites, including adenosine triphosphate (ATP), lactate, phosphoenolpyruvate (PEP), 3-phospho-D-glycerate, pyruvate, succinate, citrate, and alpha-ketoglutarate (AKG).

PET imaging

A special micro-PET/CT scanner (United Image Inc., Shanghai, China) was used for this experiment. To further explore the role of myocardial energy metabolism in the heart after CPR, the authors performed dynamic (^{18}F)-FDG PET imaging in 40 rats. The animals had fasted for 12 hours before the experiment, but they could drink water freely, and each rat was fed separately to avoid eating each other's food. Fasting blood glucose was measured in all rats via the tail vein before imaging, and the fasting blood glucose was in the range of 140–160 mg/dL. All experimental animals were administered (^{18}F)-FDG (4.63 MBq) intravenously. PET imaging of anesthetized rats (sodium pentobarbital, 45 mg/kg) was performed using a micro-PET/CT hybrid scanner. All PET images were reconstructed using two iterations of the three-dimensional ordered subset expectation-maximization algorithm (12 subsets) and 18 iterations of the accelerated version of 3D-MAP (i.e., FASTMAP), with a matrix size of 128 × 128 × 159. Attenuation correction was applied to datasets from CT images acquired just before each PET scan. No partial volume corrections were performed. Dynamic PET scans were acquired in list mode format over 90 minutes, starting just prior to the radiotracer injection. The resulting data were sorted into 0.5-mm sinogram bins and 19-time frames for image reconstruction (4 × 15 s, 4 × 60 s, 11 × 300 s). For subsequent studies, static PET scans (10 minutes) were acquired at ~70 minutes after injection of the radiotracer. PET images were analyzed by a PET radiologist and senior PET technologist with >5 years of experience in quantifying pulmonary (^{18}F)-FDG PET uptake.

Statistical analysis

IBM SPSS statistics 19.0 software (SPSS Inc., Chicago, IL, USA) was used to analyze the data. The Kolmogorov–Smirnov test was used to determine whether the data conformed to a normal distribution. Numerical variables with a normal distribution were represented as mean ± standard deviation values and categorical variables as numbers (n). A One-Way ANOVA was performed to compare more than two groups. The unpaired two-sample t-test was used for a two-group comparison. Statistical significance was defined as a two-tailed value of $P < 0.05$.

Results

The myocardial injury markers, intermediary carbohydrate metabolites of glycolysis, key intermediate products of glucose oxidation, SUVs, and cardiac dysfunction parameters of the sham, CPR, and CPR + TMZ groups are presented in Table 1. To explore the effect of energy metabolism on the heart after CPR, the authors first successfully established a rat CPR model. The serological test results showed that compared with that in the sham group, the expression of CTNI in the serum of animals after CPR increased significantly ($P = 0.014$, Figure 1a). Echocardiography and hemodynamic measurements showed that CPR treatment induced lower EF% and FS% than sham treatment ($P = 0.000$, Figure 1c, d). Meanwhile, the level of the energy metabolism marker ATP was remarkedly downregulated in the hearts of animals after CPR for 6 hours ($P = 0.01$, Figure 1b). The level of total ATP was remarkedly upregulated in the hearts of TMZ + CPR rats compared with CPR rats ($P = 0.034$, Figure 1b). Interestingly, with the increase in total ATP expression level, the tail venous blood of all rats was collected for testing, and the results showed that the CTNI level was significantly attenuated in the hearts of TMZ + CPR rats ($P = 0.021$, Figure 1a). In addition, echocardiography and hemodynamic measurements revealed that after CPR with TMZ the animals treated had higher EF% ($P = 0.065$, Figure 1c) and FS% ($P = 0.165$, Figure 1d) than those of CPR rats for 6 hours. It could be observed from the figure (Figures 1c, d) that EF% and FS% in the CPR + TMZ group were higher than the CPR group for 6 hours, but the difference was not significant after statistical analysis. This unsatisfactory result might be due to the small sample size and the short observation time. Because echocardiography and hemodynamic measurements revealed that after CPR with TMZ the rats had remarkedly higher EF% ($P = 0.026$, Figure 1c) and FS% ($P = 0.014$, Figure 1d) than the rats treated only with CPR for 24 hours. These data showed that energy metabolism was an essential factor in myocardial damage and cardiac function in the heart after CPR.

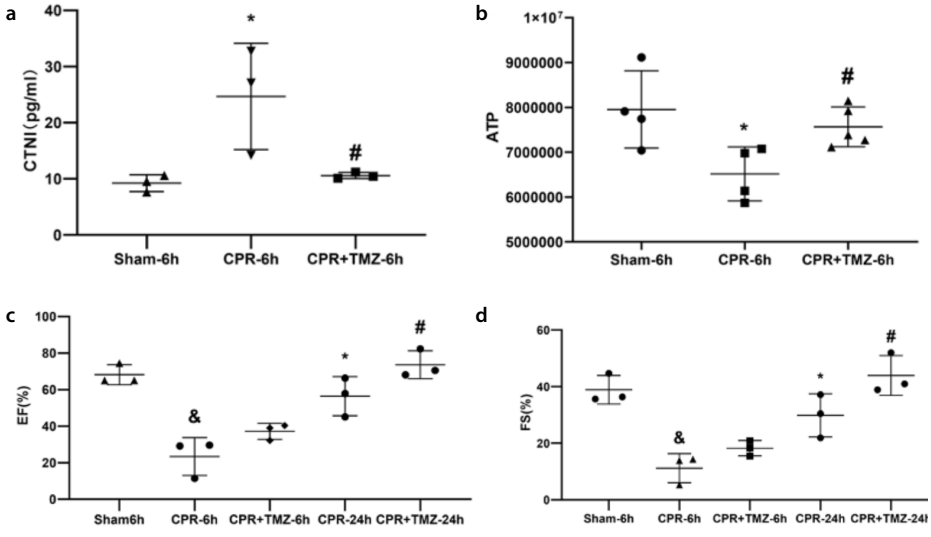

Figure 1. (a-d) Energy production and function are significantly impaired in the heart after cardiopulmonary resuscitation (CPR). **(a)** Expression levels of cardiac troponin I in the hearts of wild-type rats was detected with Assay Kit I after sham, CPR, and trimetazidine (TMZ) + CPR treatment for 6 hours (n = 4–5 rats per experimental group, #$P < 0.05$ vs. CPR 6 hours); **(b)** the results of the multiple reaction monitoring approach showed the levels of energy metabolism marker adenosine triphosphate in wild-type rats after TMZ + CPR, CPR, and sham treatment for 6 hours (n = 4–5 rats per experimental group, #$P < 0.05$ vs. CPR 6 hours); **(c, d)** Statistical results for the parameters of the echocardiographic results, including ejection fraction and fraction shortening in wild-type rats after sham surgery, CPR, and TMZ + CPR for 6 or 24 hours (n = 3 rats per experimental group, #$P < 0.05$ vs. CPR 24 hours).

Abnormal glycolysis is an important manifestation of myocardial damage after CPR.

After CPR, targeted metabolomics analysis results showed that the expression of PEP (P = 0.014, Figure 2a) and 3-phospho-D-glycerate (P = 0.000, Figure 2b) were significantly upregulated in myocardial tissue after CPR for 6 hours. And the lactate/pyruvate ratio also increased (P = 0.000, Figure 2c). The expression of AKG was significantly downregulated (P = 0.034, Figure 2d). In addition, the expression of succinate (P = 0.009, Figure 2e) and citrate (P = 0.003, Figure 2f) were significantly upregulated in myocardial tissue after CPR for 6 hours. These data suggested that glucose metabolism was altered considerably, and the degree of aerobic glucose metabolism may be significantly reduced. Nevertheless, anaerobic glycolysis may be dramatically augmented in the myocardium after CPR. In addition, TMZ treatment significantly declined the levels of PEP (P = 0.038, Figure 2a) and 3-phospho-D-glycerate (P = 0.005, Figure 2b) in the hearts of rats after CPR for 6 hours. The expression of succinate (P = 0.026, Figure 2e) and citrate (P = 0.002, Figure 2f) were significantly decreased in TMZ-treated rats after CPR for 6 hours. And the expression of AKG was significantly upregulated (P = 0.006, Figure 2d). Moreover, the lactate/pyruvate ratio also decreased (P = 0.026, Figure 2c). Furthermore, the total ATP expression was significantly increased in the hearts of TMZ-treated rats compared with control rats (P = 0.034, Figure 1b). All results comprehensively prompted that aerobic glucose metabolism may be ameliorated, but anaerobic glycolysis may be diminished in the myocardium of TMZ-treated rats after CPR. With the improvement in glucose metabolism, energy production was significantly increased in the heart after CPR. Collectively, the glucose metabolism in the myocardium was very important to myocardial energy metabolism after CPR.

To further explore the effect of glucose metabolism on the heart after CPR, the authors measured the glucose uptake of the rat heart 6 hours after CPR by the (^{18}F)-FDG PET/CT non-invasive technique. (^{18}F)-FDG PET/CT imaging showed higher FDG uptake in the heart after CPR for 6 hours compared to that in sham hearts (Figure 3a). The results showed that the value of standardized uptake value (SUV) was dramatically higher in rats after CPR for 6 hours (P = 0.000, Figure 3b). On the contrary, (^{18}F)-FDG PET/CT data showed that TMZ-treated rats after CPR for 6 hours exhibited remarkedly lower FDG uptake and SUV values (P = 0.000, Figure 3a and b).

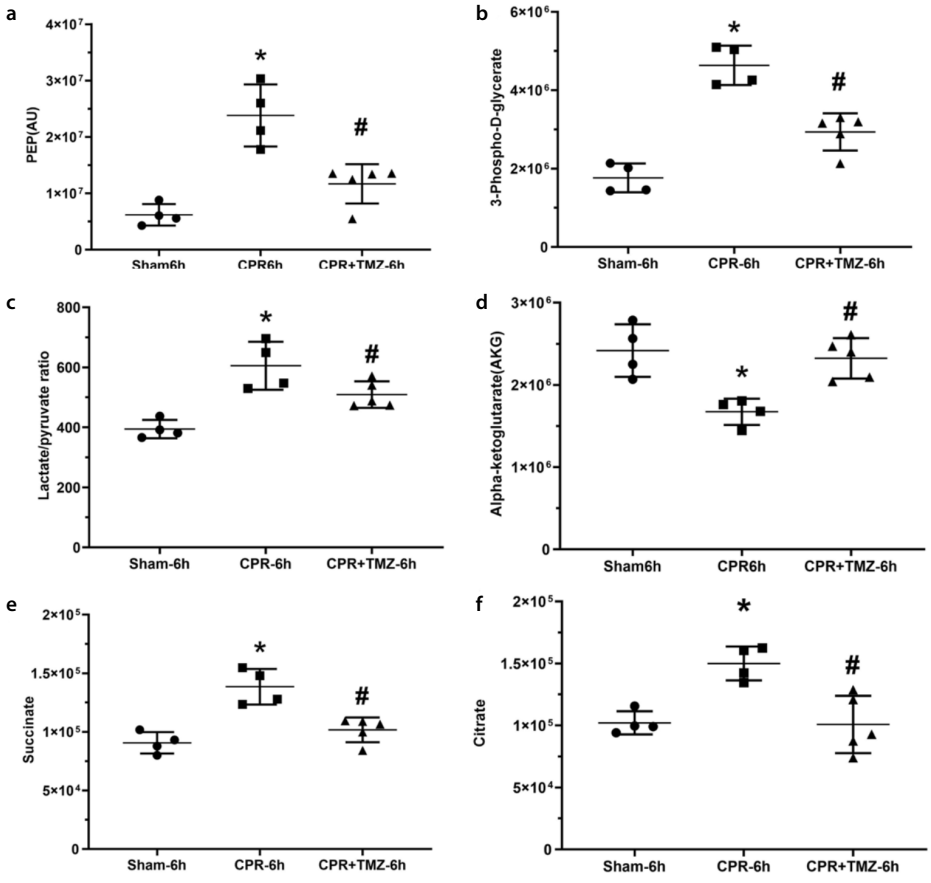

Figure 2. (a-f) Glucose uptake and abnormal glycolysis are significantly enhanced in the animal heart after cardiopulmonary resuscitation (CPR). **(a, b)** Expression levels of phosphoenolpyruvate and 3-phospho-D-glycerate were increased in the hearts of wild-type rats, detected with the multiple reaction monitoring (MRM) approach after sham, CPR, and trimetazidine (TMZ) + CPR surgery for 6 hours (n = 4–5 rats per experimental group, #P < 0.05 vs. CPR 6 hours); **(c)** the lactate/pyruvate ratio was detected after sham, CPR, and TMZ + CPR surgery for 6 hours. (n = 4–5 rats per experimental group, #P < 0.05 vs. CPR 6 hours); **(d-f)** The results of the MRM approach showed the expression of alpha-ketoglutarate, succinate, and citrate in Sprague-Dawley rats' hearts after sham, CPR, and TMZ + CPR treatment for 6 hours. (n = 4–5 rats per experimental group, #P < 0.05 vs. CPR 6 hours).

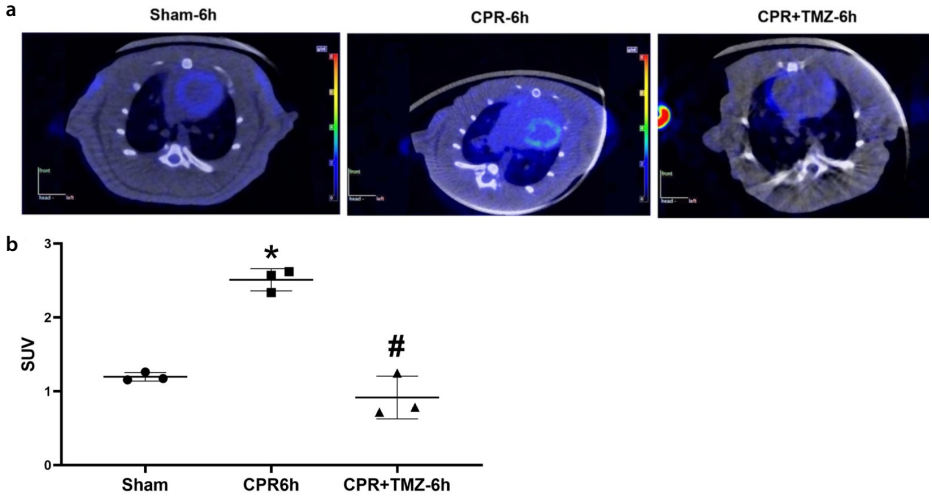

Figure 3. (a, b) (^{18}F)-fluoro-D-glucose (FDG) positron emission tomography/computed tomography [(^{18}F)-FDG PET/CT] can monitor the changes in cardiac function and myocardial energy metabolism after cardiopulmonary resuscitation (CPR) by tracking glucose metabolism. **(a)** (^{18}F)-FDG PET/CT imaging showed FDG uptake after sham, CPR, and trimetazidine (TMZ) + CPR treatment for 6 hours (n = 3 rats per experimental group, #P < 0.05 vs. CPR 6 hours); **(b)** Statistical results for the value of standardized uptake value in the hearts of TMZ-treated wild-type rats after CPR or sham treatment for 6 hours (n = 3 rats per experimental group, #P < 0.05 vs. CPR 6 hours).

Discussion

In this research, the authors' findings showed that the non-invasive (^{18}F)-FDG PET/CT technology could predict early changes in myocardial damage and cardiac function by tracking glucose metabolism in the heart after CPR. In the initial stage of the experiment, the authors successfully established a rat CPR model and found that the total ATP decreased significantly in the heart after CPR. This finding suggested that myocardial energy metabolism was dysfunctional after CPR. Furthermore, myocardial damage was aggravated, and heart function was significantly attenuated with decreased ATP expression levels. Subsequently, the authors tested the important intermediate products of aerobic oxidation and anaerobic glycolysis of glucose. As a result, it was found that the aerobic oxidation of glucose may be reduced, and anaerobic glycolysis may be significantly enhanced in the myocardium in the early stage of CPR. The authors used TMZ to increase the aerobic oxidation of glucose to further clarify the role of glucose metabolism in the myocardium after CPR. The results revealed that myocardial damage was also significantly reduced, and cardiac function was significantly improved with the significantly increased ATP levels. These data indicate that the functional status of the myocardium after CPR was closely related to glucose metabolism. Therefore, the authors successfully tracked the changes in glucose metabolism and cardiac function in the heart after CPR through the measurement of the myocardial glucose uptake rate and the SUV value by (^{18}F)-FDG PET/CT.

In the past decades, many studies have shown that glucose and fatty acids are im-

Table 1. Comparison of the myocardial injury marker, intermediary carbohydrate metabolites of glycolysis, key intermediate products of glucose oxidation, SUVs, and cardiac dysfunction between the groups

Variable	Groups					*P*
Myocardial injury marker	Sham (Mean ± SD)		CPR 6 h (Mean ± SD)		CPR + TMZ 6 h (Mean ± SD)	
CTNI	9.25 ± 1.49		24.69 ± 9.49		10.59 ± 0.55	Sham vs. CPR 6 h, 0.014 CPR 6 h vs. CPR + TMZ 6 h, 0.021
The intermediary carbohydrate metabolites of glycolysis						
PEP	6180136.89 ± 1903793.06		23823999.4 ± 5506351.51		11686084.23 ± 3499530.67	Sham vs. CPR 6 h, 0.014 CPR 6 h vs. CPR + TMZ 6 h, 0.038
3-phospho-D-glycerate	1763595.05 ± 267659.74		4636341.47 ± 502118.8		2937035.57 ± 474740.75	Sham vs. CPR 6 h, 0.000 CPR 6 h vs. CPR + TMZ 6 h, 0.005
Lactate/pyruvate ratio	394.19 ± 30.62		605.2 ± 80.13		509.18 ± 44.22	Sham vs. CPR 6 h, 0.000 CPR 6 h vs. CPR + TMZ 6 h, 0.026
The key intermediate products of glucose oxidation						
AKG	2418330.11 ± 319828.6		1673549.55 ± 160275.97		2324160.51 ± 245632.42	Sham vs. CPR 6 h, 0.034 CPR 6 h vs. CPR + TMZ 6 h, 0.006
Citrate	102137.4 ± 9345.74		150015.51 ± 13696.5		100833 ±23156.7	Sham vs. CPR 6 h, 0.003 CPR 6 h vs. CPR + TMZ 6 h, 0.002
Succinate	90700.06 ± 9145.65		138561.3 ± 15226.47		101777.62 ± 10572.9	Sham vs. CPR 6 h, 0.009 CPR 6 h vs. CPR + TMZ 6 h, 0.026
Energy marker						
The total ATP	7953685.05 ± 861412.36		6515711.65 ± 600582.21		7566185.2 ± 444470.3	Sham vs. CPR 6 h, 0.001 CPR 6 h vs. CPR + TMZ 6 h, 0.034
(^{18}F)-FDG PET/CT						
SUV	1.20 ± 0.06		2.51 ± 0.15		0.92 ± 0.29	Sham vs. CPR 6 h, 0.000 CPR 6 h vs. CPR + TMZ 6 h, 0.000
Variable	**Groups**					
Cardiac dysfunction	**Sham (Mean ± SD)**	**CPR 6 h (Mean ± SD)**	**CPR + TMZ 6 h (Mean ± SD)**	**CPR 24 h (Mean ± SD)**	**CPR + TMZ 24 h (Mean ± SD)**	***P***
EF	68.17 ± 5.49	23.39 ± 10.35	37.19 ± 4.37	56.39 ± 10.68	73.62 ± 7.6	Sham vs. CPR 6 h, 0.000 CPR 24 h vs. CPR + TMZ 6 h, 0.026
FS	38.88 ± 5.04	11.15 ± 5.13	18.22 ± 2.71	29.83 ± 7.65	43.91 ± 7.02	Sham vs. CPR 6 h, 0.000 CPR 24 h vs. CPR + TMZ 6 h, 0.014

TMZ, trimetazidine; SD, standard deviation; CTNI, cardiac troponin I; PEP, phosphoenolpyruvate; AKG, alpha-ketoglutarate; SUV, standardized uptake value; EF, ejection fraction; FS, fraction shortening; ATP, adenosine triphosphate; CPR, cardiopulmonary resuscitation; (^{18}F)-FDG PET/CT, (^{18}F)-fluoro-D-glucose positron emission tomography/computed tomography

portant energy substrates for myocardial metabolism. Sixty to seventy percent of the energy required for cardiac contraction in myocardial metabolism is mainly generated by the oxidative metabolism of fatty acids.[7,18,19] The rest of the energy was mainly derived from the supply of aerobic oxidation of glucose. However, the effects of changes in glucose metabolism in the myocardium after CPR remains poorly understood. It is well known that the most important metabolism of glucose is the decomposition into PEP, 3-phospho-D-glycerate, and pyruvate through glycolysis. Then, under aerobic conditions, pyruvate enters the tricarboxylic acid cycle and gradually produces AKG, succinic acid, citrate, etc., producing more ATP in this process. Under anaerobic conditions, pyruvate enters the anaerobic glycolysis pathway to generate lactic acid and less ATP. Studies have also shown that the level of myocardial ATP is closely related to myocardial cell damage and has a positive correlation with myocardial contractile energy.[20] Various factors, such as myocardial ischemia-reperfusion injury caused by energy metabolism disorders after CPR, could lead to severe systolic dysfunction,[21,22] and the severity of this injury directly determines the patient's prognosis.[23] Consistent with the results of these studies, the authors found that the lactate/pyruvate ratio was significantly increased; in contrast, the level of AKG was significantly downregulated, while succinate and citrate were considerably upregulated increased in myocardial tissue after CPR. The increase in succinate and citrate after CPR was also a manifestation of mitochondrial energy metabolism disorder. This disorder was related to the increase in reactive oxygen species generated from myocardial oxidative stress after CPR. This result showed that the role of anaerobic glycolysis in the energy supply of the myocardium might be greatly enhanced and the level of aerobic oxidation of glucose may be significantly reduced in the heart after CPR. The authors also found that PEP and 3-phospho-D-glycerate in the rat myocardium were significantly increased, indicating that glucose uptake in the myocardium was enhanced after CPR. Consistent with Liu et al.[24] research results, glucose uptake in myocardial ischemia and hypoxia was also ameliorated, even after the myocardial blood flow was restored. Although the authors test results showed that the total ATP level in the rat myocardium was significantly reduced compared to that in the sham group, myocardial glucose uptake was increased after CPR. This result suggested that the total energy supply to the myocardium was decreased, but the metabolism of glucose also underwent adaptive changes after CPR.

Interestingly, the myocardial injury marker CTNI was upregulated significantly, and the left ventricular function of the animal heart also deteriorated significantly with the downregulation in ATP. As mentioned above, myocardial damage and cardiac function changes were closely related to myocardial energy metabolism. After CPR, glucose metabolism in the myocardium also showed significant adaptive changes. These findings suggested that glucose metabolism might play an important role in CPR.

To further clarify the relationship between glucose metabolism and myocardial damage and cardiac function after CPR, TMZ, a regulator to improve the aerobic oxidation of myocardial glucose, was applied in this experiment.[25,26] TMZ mainly optimized the oxygen utilization process in the cell mitochondrial matrix and inhibited 3-KAT function while enhancing the activity of pyruvate dehydrogenase to amplify the aerobic oxidation of glucose to ultimately optimize the energy supply of cardiomyocytes.[27-30] The authors' research results showed that the expression levels of intermediates (AKG, succinate, and citrate) of the tricarboxylic acid cycle were very close to those of the sham group, and the anaerobic glycolysis marker (the ratio of lactic acid to pyruvate) was significantly decreased in the TMZ intervention group compared with the CPR group. And the expression of ATP in the TMZ + CPR group was significantly upregulated. Surprisingly, with the increase in ATP expression levels, myocardial damage and cardiac function were also significantly improved. There was a negative correlation between energy metabolism and myocardial injury. Hence, enhanced anaerobic glycolysis after CPR played a role in protecting the myocardium.

In addition, it was interesting that the authors' study revealed that the expression levels of PEP and 3-phospho-D-glycerate in the TMZ + CPR group were significantly lower than those in the CPR group. This result suggested that myocardial glucose uptake was reduced in the TMZ + CPR group. Hence, the authors found that the myocardial glucose uptake rate could be used to predict or assist in monitoring the changes in myocardial injury and cardiac function after CPR. Furthermore, the laboratory and cardiac ultrasound data collected in this study also supported this hypothesis.

The authors realized the importance of glucose metabolism to the myocardium after CPR through the above series of experiments. Then, the authors further explored the possibility of basic theoretical research that could be applied to the clinic. (^{18}F)-FDG PET/CT technology was used to track the footprint of glucose metabolism in cardiomyocytes. (^{18}F)-FDG is a radionuclide fluorine-labeled deoxyglucose that can track the initial processes involved in glucose metabolism, including glucose transmembrane transport and hexokinase-regulated phosphorylation in the heart.[31] In myocardial cells, (^{18}F)-FDG is phosphorylated into (^{18}F)-FDG-6-phosphate, and the dephosphorylation process of FDG-6-phosphate is very slow. It does not easily pass through the cell membrane and is not further metabolized through glycogen synthesis and catabolism to stay in cardiomyocytes.[13] Therefore, the glucose metabolism of the myocardium could be measured by FDG PET imaging. In the authors' experiment, the (^{18}F)-FDG PET/CT results showed that the SUV value and FDG uptake after CPR were significantly higher than those of the control group. At the same time, the experimental group treated with TMZ had the opposite result.

In clinical diagnosis and treatment, the prognosis for patients after CPR is closely related to the location, scope, and degree of myocardial injury. The traditional blood test is affected by many factors and can only evaluate the degree of myocardial injury, while the location and scope of myocardial injury cannot be accurately evaluated. (^{18}F)-FDG PET/CT a non-invasive technology, can directly determine the location and scope of myocardial injury by monitoring glucose metabolism changes in the myocardium to more accurately evaluate the prognosis and risk of patients after CPR. It is also possible that the changes in myocardial metabolism may be earlier than the abnormalities of myocardial blood perfusion. In this case, an earlier warning can be achieved through (^{18}F)-FDG PET/CT technology before traditional examinations find myocardial damage and changes in cardiac function, thereby enabling early treatment and possibly improving prognosis.

There were some limitations to the authors' study. First, the myocardial glucose uptake can be affected by the levels of insulin, fatty acids, and other substances. Any follow-up study needs to increase the number of samples and evaluate the factors affecting the (^{18}F)-FDG uptake. Second, there was a certain proportion of CPR patients with diabetes. Such samples were not included in this study. Follow-up studies are needed to establish a CPR model with diabetes and

analyze the myocardial (^{18}F)-FDG uptake of diabetes patients. Last, most medical institutions do not have the conditions for PET/CT. Therefore, the authors can explore the relationship between magnetic resonance imaging or Doppler echocardiography and myocardial energy metabolism.

In conclusion, the present study confirms that anaerobic glycolysis acted as a protector in the heart after CPR, and the improvement in aerobic metabolism of glucose could attenuate myocardial damage after CPR. Glucose metabolism plays an important role in myocardial tissue repair after CPR. As a non-invasive imaging technique, (^{18}F)-FDG PET/CT can track the footprint of glucose metabolism to evaluate the functional status of cardiomyocytes after CPR, which helps to better guide clinical treatment and prognostic evaluation.

Conflict of interest disclosure

The authors declared no conflicts of interest.

Funding

National Natural Science Youth Foundation of China (no: 81701871).

References

1. Mehaffey JH, Money D, Charles EJ, et al. Adenosine 2A receptor activation attenuates ischemia reperfusion injury during extracorporeal cardiopulmonary resuscitation. *Ann Surg*. 2019;269(6):1176-1183. [CrossRef]
2. Matsuura TR, Bartos JA, Tsangaris A, et al. Early effects of prolonged cardiac arrest and ischemic postconditioning during cardiopulmonary resuscitation on cardiac and brain mitochondrial function in pigs. *Resuscitation*. 2017;116:8-15. [CrossRef]
3. Zhang Y, Song Y, Shu T, Liang L, Shao W, Guo L, Sun P. Ultrasound improves the outcomes of cardiopulmonary resuscitation in rats by stimulating the cholinergic anti-inflammatory pathway. *Mol Med Rep*. 2019;20(3):2675-2684. [CrossRef]
4. Ulmer BM, Stoehr A, Schulze ML, et al. Contractile work contributes to maturation of energy metabolism in hiPSC-derived cardiomyocytes. *Stem Cell Reports*. 2018;10(3):834-847. [CrossRef]
5. Ulmer BM, Eschenhagen T. Human pluripotent stem cell-derived cardiomyocytes for studying energy metabolism. *Biochim Biophys Acta Mol Cell Res*. 2020;1867(3):118471. [CrossRef]
6. Piquereau J, Ventura-Clapier R. Maturation of cardiac energy metabolism during perinatal development. *Front Physiol*. 2018;9:959. [CrossRef]
7. Heather LC, Howell NJ, Emmanuel Y, Cole MA, Frenneaux MP, Pagano D, Clarke K. Changes in cardiac substrate transporters and metabolic proteins mirror the metabolic shift in patients with aortic stenosis. *PLoS One*. 2011;6(10):e26326. [CrossRef]
8. Tran DH, Wang ZV. Glucose metabolism in cardiac hypertrophy and heart failure. *J Am Heart Assoc*. 2019;8(12):e012673. [CrossRef]
9. Hackenhaar FS, Medeiros TM, Heemann FM, et al. Therapeutic hypothermia reduces oxidative damage and alters antioxidant defenses after cardiac arrest. *Oxid Med Cell Longev*. 2017;2017:8704352. [CrossRef]
10. Tournier N, Saba W, Goutal S, et al. Influence of P-glycoprotein inhibition or deficiency at the blood-brain barrier on (18)F-2-fluoro-2-deoxy-D-glucose ((18)F-FDG) brain kinetics. *AAPS J*. 2015;17(3):652-659. [CrossRef]
11. Dou KF, Gao XJ, Xie BQ, Li Y, He ZX, Yang MF. Dual-time-point myocardial 18F-FDG imaging in the detection of coronary artery disease. *BMC Cardiovasc Disord*. 2017;17(1):120. [CrossRef]
12. Rahman WT, Wale DJ, Viglianti BL, et al. The impact of infection and inflammation in oncologic 18F-FDG PET/CT imaging. *Biomed Pharmacother*. 2019;117:109168. [CrossRef]
13. Skali H, Schulman AR, Dorbala S. 18F-FDG PET/CT for the assessment of myocardial sarcoidosis. *Curr Cardiol Rep*. 2013;15(4):352. [CrossRef]
14. Chung YH, Lu KY, Chiu SC, et al. early imaging biomarker of myocardial glucose adaptations in high-fat-diet-induced insulin resistance model by using 18F-FDG PET and [U-13C]glucose nuclear magnetic resonance tracer. *Contrast Media Mol Imaging*. 2018;2018:8751267. [CrossRef]
15. Wang P, Yao L, Zhou LL, et al. Carbon monoxide improves neurologic outcomes by mitochondrial biogenesis after global cerebral ischemia induced by cardiac arrest in rats. *Int J Biol Sci*. 2016;12(8):1000-1009. [CrossRef]
16. Fu ZY, Wu ZJ, Zheng JH, Qin T, Yang YG, Chen MH. The incidence of acute kidney injury following cardiac arrest and cardiopulmonary resuscitation in a rat model. *Ren Fail*. 2019;41(1):278-283. [CrossRef]
17. Schroeder DC, Maul AC, Mahabir E, et al. Evaluation of small intestinal damage in a rat model of 6 Minutes cardiac arrest. *BMC Anesthesiol*. 2018;18(1):61. [CrossRef]
18. Carolo dos Santos K, Pereira Braga C, Octavio Barbanera P, Seiva FR, Fernandes Junior A, Fernandes AA. Cardiac energy metabolism and oxidative stress biomarkers in diabetic rat treated with resveratrol. *PLoS One*. 2014;9(7):e102775. [CrossRef]
19. Li F, Li J, Li S, Guo S, Li P. Modulatory effects of chinese herbal medicines on energy metabolism in ischemic heart diseases. *Front Pharmacol*. 2020;11:995. [CrossRef]
20. Mijailovich SM, Nedic D, Svicevic M, et al. Modeling the actin.myosin ATPase cross-bridge cycle for skeletal and cardiac muscle myosin isoforms. *Biophys J*. 2017;112(5):984-996. [CrossRef]
21. Anderson RJ, Jinadasa SP, Hsu L, et al. Shock subtypes by left ventricular ejection fraction following out-of-hospital cardiac arrest. *Crit Care*. 2018;22(1):162. [CrossRef]
22. Yang CF. Clinical manifestations and basic mechanisms of myocardial ischemia/reperfusion injury. *Ci Ji Yi Xue Za Zhi*. 2018;30(4):209-215. [CrossRef]
23. Zhao ZG, Tang ZZ, Zhang WK, Li JG. Protective effects of embelin on myocardial ischemia-reperfusion injury following cardiac arrest in a rabbit model. *Inflammation*. 2015;38(2):527-533. [CrossRef]
24. Liu Z, Chen JM, Huang H, et al. The protective effect of trimetazidine on myocardial ischemia/reperfusion injury through activating AMPK and ERK signaling pathway. *Metabolism*. 2016;65(3):122-130. [CrossRef]
25. Dehina L, Vaillant F, Tabib A, et al. Trimetazidine demonstrated cardioprotective effects through mitochondrial pathway in a model of acute coronary ischemia. Naunyn Schmiedebergs *Arch Pharmacol*. 2013;386(3):205-215. [CrossRef]
26. Chrusciel P, Rysz J, Banach M. Defining the role of trimetazidine in the treatment of cardiovascular disorders: some insights on its role in heart failure and peripheral artery disease. *Drugs*. 2014;74(9):971-980. [CrossRef]
27. Kantor PF, Lucien A, Kozak R, Lopaschuk GD. The antianginal drug trimetazidine shifts cardiac energy metabolism from fatty acid oxidation to glucose oxidation by inhibiting mitochondrial long-chain 3-ketoacyl coenzyme A thiolase. *Circ Res*. 2000;86(5):580-588. [CrossRef]
28. Fragasso G, Spoladore R, Cuko A, Palloshi A. Modulation of fatty acids oxidation in heart failure by selective pharmacological inhibition of 3-ketoacyl coenzyme-A thiolase. *Curr Clin Pharmacol*. 2007;2(3):190-196. [CrossRef]
29. Jain D, He ZX, Lele V, Aronow WS. Direct myocardial ischemia imaging: a new cardiovascular nuclear imaging paradigm. *Clin Cardiol*. 2015;38(2):124-130. [CrossRef]
30. Ramezani-Aliakbari F, Badavi M, Dianat M, Mard SA, Ahangarpour A. The effects of trimetazidine on QT-interval prolongation and cardiac hypertrophy in diabetic rats. *Arq Bras Cardiol*. 2019;112(2):173-178. [CrossRef]
31. Daly KP, Dearling JL, Seto T, Dunning P, Fahey F, Packard AB, Briscoe DM. Use of [18F]FDG positron emission tomography to monitor the development of cardiac allograft rejection. *Transplantation*. 2015;99(9):e132-e139. [CrossRef]